Monthly Notices
of the
ROYAL ASTRONOMICAL SOCIETY

MNRAS **503,** 1–12 (2021)
Advance Access publication 2021 February 3

doi:10.1093/mnras/stab281

Neutron stars mergers in a stochastic chemical evolution model: impact of time delay distributions

L. Cavallo,[1]★ G. Cescutti[2,3] and F. Matteucci[1,2,4]

[1]*Dipartimento di Fisica, Sezione di Astronomia, Università di Trieste, Via G. B. Tiepolo 11, I-34143 Trieste, Italy*
[2]*INAF, Osservatorio Astronomico di Trieste, Via G. B. Tiepolo 11, I-34143 Trieste, Italy*
[3]*IFPU, Istitute for the Fundamental Physics of the Universe, Via Beirut, 2, I-34151 Trieste, Italy*
[4]*INFN, Sezione di Trieste, Via A. Valerio 2, I-34127 Trieste, Italy*

Accepted 2021 January 25. Received 2020 December 26; in original form 2020 April 29

ABSTRACT

We study the evolution of the [Eu/Fe] ratio in the Galactic halo by means of a stochastic chemical evolution model considering merging neutron stars as polluters of europium. We improved our previous stochastic chemical evolution model by adding a time delay distribution for the coalescence of the neutron stars, instead of constant delays. The stochastic chemical evolution model can reproduce the trend and the observed spread in the [Eu/Fe] data with neutron star mergers as unique producers if we assume: (i) a delay time distribution $\propto t^{-1.5}$, (ii) an $M_{\rm Eu} = 3 \times 10^{-6}\,{\rm M}_{\odot}$ per event, (iii) progenitors of neutron stars in the range 9–50 $\rm M_{\odot}$, and (iv) a constant fraction of massive stars in the initial mass function (0.02) that produce neutron star mergers. Our best model is obtained by relaxing point (iv) and assuming a fraction that varies with metallicity. We confirm that the mixed scenario with both merging neutron stars and supernovae as europium producers can provide a good agreement with the data relaxing the constraints on the distribution time delays for the coalescence of neutron stars. Adopting our best model, we also reproduce the dispersion of [Eu/Fe] at a given metallicity, which depends on the fraction of massive stars that produce neutron star mergers. Future high-resolution spectroscopic surveys, such as 4MOST and WEAVE, will produce the necessary statistics to constrain at best this parameter.

Key words: nuclear reactions, nucleosynthesis, abundances – stars: abundances – binaries: close – stars: neutron – Galaxy: evolution – Galaxy: halo.

1 INTRODUCTION

The majority of all nuclei that are heavier than the iron-peak element ($A \geq 70$) are produced by neutron capture reactions. The neutron capture processes are divided into two different classes: rapid or r-process (neutron capture time-scale shorter than β decay) and slow or s-process (in this case the neutron capture time-scale is longer than β decay). Most neutron capture elements are produced by both r- and s-process, but for some of these heavy nuclei, the production is dominated by only one process. A series of works found a spread of r-process elements in the metal-poor environment of the Galactic halo (McWilliam 1998; Fulbright 2000; Koch & Edvardsson 2002; Honda et al. 2004). This spread can reach 2 dex at [Fe/H] ~ -3 dex. On the other hand, [α/Fe] ratios (where α stands for α-elements) show a smaller scatter than r-process elements. The α-element spread, if real and not due to observational uncertainties, can be due to cosmic selection effects favoring contributions from supernovae (SNe) in a certain mass range (see Ishimaru et al. 2003; Karlsson & Gustafsson 2005). In literature Eu is often indicated as a good r-process tracer for two basic reasons: (i) more than 90 per cent of Eu in the Solar system has been produced by r-process (Cameron 1982; Howard et al. 1986; Bisterzo et al. 2015). (ii) Europium is one of the few r-process elements that shows clean atomic lines in the visible part of the electromagnetic spectrum, and this makes Eu abundances easier to measure than other r-process elements (Woolf, Tomkin & Lambert 1995).

Two main astrophysical sites have been proposed for Eu production: (i) core-collapse SNe (Type II SNe during explosive nucleosynthesis (Cowan, Thielemann & Truran 1991; Woosley et al. 1994; Wanajo et al. 2001). However, there are still many uncertainties in the physical mechanism involved in Eu production in Type II SNe (Arcones, Janka & Scheck 2007). (ii) neutron star mergers (NSM) can provide a strong Eu production (Symbalisty & Schramm 1982; Freiburghaus, Rosswog & Thielemann 1999; Oechslin, Janka & Marek 2007; Panov, Korneev & Thielemann 2008; Bauswein, Goriely & Janka 2013; Hotokezaka et al. 2013; Perego et al. 2014; Wanajo et al. 2014). Each event can produce a total amount of Eu from 10^{-7} to $10^{-5}\,{\rm M}_{\odot}$ (Korobkin et al. 2012).

Previous models, such as Argast et al. (2004), computed the evolution of Eu for the halo of our Galaxy with an in-homogeneous chemical evolution model. They concluded that NSMs cannot be the major production site of Eu due to their low merging rate. In this scenario NSMs failed to reproduce the observation of stars at low metallicity ([Fe/H] < -2.5). Later Cescutti et al. (2006) found that in a model with instantaneous mixing, SNe II can be entirely responsible for the production of Eu. Moreover, he suggested that Eu originates from stars in a mass range 12–30 $\rm M_{\odot}$.

★ E-mail: cavallo.lorenzo@outlook.com

© 2021 The Author(s)
Published by Oxford University Press on behalf of Royal Astronomical Society

Downloaded from https://academic.oup.com/mnras/article/503/1/1/6127305 by inaf user on 05 August 2021

Matteucci et al. (2014) showed that in a chemical model with instantaneous mixing approximation (I.M.A), neutron stars (NS) can be the only production site of Eu under some conditions: the time-scale of coalescence cannot be longer than 1 Myr; the yield of Eu per single event is around 3×10^{-6} $M_{\odot}$; the mass range of neutron stars progenitors is 9–50 $M_{\odot}$. With similar assumptions on NSM parameters, Cescutti et al. (2015) proved that with a stochastic chemical evolution model these events can also explain the large spread of [Eu/Fe] versus [Fe/H] observed in the halo of our Galaxy. It was also found out that the scenario that best reproduces the observational data is the one where both neutron star mergers and a fraction of Type II SNe produce Eu. A main assumption of the previous models is the short coalescence time of NS systems, but some observational bounds cannot be satisfied by a constant and short coalescence time, such as to explain the recently observed event GW170817 which occurred in an early-type galaxy with no star formation, as well as to reproduce the cosmic rate of short gamma-ray bursts (short-GRBs). Recently Côté et al. (2019) proved that, if we assume NSM as the only r-process site, there are some tensions between models and observational data when we drop the condition of short and constant coalescence time. In particular, they found that NSMs with a coalescence time that follows the same delay time distribution (DTD) of SNe Ia cannot reproduce the decreasing trend of [Eu/Fe] at [Fe/H] > -1 dex in the Galactic disc. However, Schönrich & Weinberg (2019) showed that, also with a DTD for NSM (with a characteristic merger time-scale $t_{\rm NS}$ = 150 Myr), they were able to explain the observed abundance patterns assuming a 2-phase interstellar medium (ISM; hot and cold). On the other hand, Simonetti et al. (2019) adopted a DTD for NSM built from theoretical considerations and concluded that either SNe II or a fraction of NSM variable in time can potentially explain the [Eu/Fe] in the Galaxy as well as the cosmic rate of short-GRBs.

Moreover, the effect of a DTD for NSM on the chemical evolution of r-process elements was also explored by Shen et al. (2015). In particular, they investigated the chemical evolution of the heavy r-process elements in our Galaxy using a high-resolution cosmological simulation (Eris) for the formation of a Milky Way like galaxy. They used a power-law slope with two different exponents: $\propto t^{-x}$ ($x = 1; 2$). Later, in the framework of the hierarchical galaxy formation, Komiya & Shigeyama (2016) explored the effects of propagation of NSM ejecta across proto-galaxies on the r-process chemical evolution. Considering these effects, they found that NSMs with a DTD are able to reproduce the emergence of r-process elements at very low metallicity ([Fe/H] ~ -3 dex).

In this paper, we want to test whether NSM with coalescence time that follows a proper DTD can explain the spread of [Eu/Fe] of metal-poor stars ([Fe/H] < -1) in the Galactic halo. To compute the chemical enrichment we adopt a stochastic chemical evolution model, proposed in Cescutti (2008), that mimics an in-homogeneous mixing thanks to a stochastic modelling. We also explore cases in which both NSM (with a DTD) and Type II SNe produce Europium. In particular, in the last part of the work, we take into account the contribution of magneto-rotationally driven (MRD) SNe in the Eu enrichment. MRD SNe (Winteler et al. 2012; Mösta et al. 2015; Nishimura, Takiwaki & Thielemann 2015) have been indicated as a promising source of r-process in the early Galaxy (Cescutti & Chiappini 2014).

The paper is organized as follows: in Section 2, we describe the observations; in Section 3, we introduce the adopted chemical evolution model. In Section 4, we discuss our results and finally in Section 5, we draw some conclusions.

2 OBSERVATIONAL CONSTRAINTS

2.1 [Eu/Fe] of metal-poor stars in the Galactic halo

The abundances measured in halo stars show a clear large scatter in the ratio of [r/Fe], where r stands for an r-process element, versus metallicity. Cescutti (2008) suggested that the wider spread observed in neutron-capture elements, compared to [α/Fe] ratios, is a consequence of the difference in mass ranges between the production sites. This also implies that, in the early Universe, the production of Eu must have been rare and prolific compared to the one of α-elements. To test the predictions of our model, we use the abundances of the halo stars contained in Roederer et al. (2014). In this data base, we have found europium abundances of 115 metal-poor stars. We chose to test our models with a data set provided by a single author even if the dimension of the sample is quite small compared to the total amount of data that are available in literature ($\simeq$400), e.g. JINAbase (Abohalima & Frebel 2018). We have opted for this choice in order to remove potential off-sets between different data. We have also noted that there is a not negligible off-set of about 0.2–0.3 dex towards lower [Fe/H], compared to the abundances obtained for common stars by other authors (see table 9, Roederer et al. 2014).

2.2 Neutron star mergers as progenitors of short gamma-ray bursts

Gamma-ray bursts display a bi-modal duration distribution with a separation between the short and long-duration bursts at about 2 s. The progenitors of long GRBs have been identified as massive stars. On the other hand, short-GRBs are thought to be correlated with compact object mergers (Eichler et al. 1989; Tanvir et al. 2013; Berger 2014). This hypothesis has been recently reinforced by the observation of a short GRB that followed the NSM event GW170817 detected by LIGO/Virgo Collaboration (Abbott et al. 2017b). In particular, NGC 4993, the host galaxy of GW170817, is an early-type galaxy (Abbott et al. 2017a; Coulter et al. 2017). If we assume a coalescence time constant and short, at least $<$10 Myr as suggested in Matteucci et al. (2014) and Cescutti et al. (2015), it will be impossible to detect an NSM in an early-type galaxy, where the star formation is over and all the NS–NS systems should have already merged. This requires the adoption of a DTD including long time-scales. As a caveat, we should also point out that it is not impossible that the merger took place in a dwarf galaxy still star forming that we are unable to distinguish.

3 THE CHEMICAL EVOLUTION MODEL

The chemical evolution model adopted here is the same as in Cescutti et al. (2015), which is based on the stochastic model developed by Cescutti (2008). We review its main characteristics to improve the reader comprehension of the work.

The Galactic halo is simulated by means of 200 stochastic realizations. Each realization consists of a non-interacting region with the same typical volume. The dimensions of the typical volume were chosen in order to neglect the interactions between different regions. In fact, for typical ISM densities, an SN remnant becomes indistinguishable from the ISM before reaching $\sim$50 pc (Thornton et al. 1998). On the other hand, we do not want a too large volume because in that case, we would lose the stochasticity. For these reasons has been chosen a typical volume with a surface of 40000 pc^2. This area is slightly higher compared to original one adopted in Cescutti (2008), but still within the acceptable dimension

Downloaded from https://academic.oup.com/mnras/article/503/1/1/6127305 by inaf user on 05 August 2021

for an SN bubble in a low-density and low-metallicity environment. This increased surface promotes a first enrichment at slightly lower [Fe/H], better matching the slightly more metal-poor data used. We consider 200 realizations to ensure a good statistical sample.

The model uses time-steps of 1 Myr, which is shorter than any stellar lifetime considered in this model; the minimum lifetime is, in fact, 3 Myr for an 80 $M_\odot$ star, which is the maximum stellar mass considered.

In each region, following the homogeneous model by Chiappini et al. (2008), we assume the following function for the infall of gas with primordial composition

$$\frac{\mathrm{d}Gas_{\rm in}(t)}{\mathrm{d}t} = I_{\rm nfall} \mathrm{e}^{-(t-t_0)^2/2\sigma_0^2}, \quad (1)$$

where t_0 is set to 100 Myr, σ_0 is 50 Myr, and $I_{\rm nfall}$ is equal to 1.28×10^4 $M_\odot$ Myr^{-1}. We define the star formation rate (SFR) as

$$\mathrm{SFR}(t) = \nu \left(\frac{\sigma_{\rm gas}(t)}{\sigma_{\rm h}} \right)^{1.5}, \quad (2)$$

where $\sigma_{\rm gas}(t)$ is the surface density of the gas inside a volume at each time-step, $\sigma_{\rm h} = 80$ $M_\odot$ pc^{-2} and ν is set to 2862 $M_\odot$ Myr^{-1} . We also take into account an outflow that follows the law

$$\frac{\mathrm{d}Gas_{\rm out}(t)}{\mathrm{d}t} = \mathrm{Wind} * \mathrm{SFR}(t), \quad (3)$$

where Wind is set to 8.

In all the subhaloes of the model, we assume the same SFR and infall laws. The following lines will introduce the stochastic part contained in our model.

Let us assume that we know the mass that is transformed at each time-step into stars ($M^{\rm new}_{\rm stars}$), then we generate one star with a mass sorted out with a random function, weighted on the initial mass function (IMF) of Scalo (1986) in the mass range from 0.1 to 100 $M_\odot$. After that, the mass of the second star is extracted, and so on until the total mass of newborn stars reaches $M^{\rm new}_{\rm stars}$. In this way, the total amount of mass transformed into new stars is the same in each region at each time-step, but the total number and mass distribution of stars are different. For all the stars we also know mass and lifetime. In particular, we assume the stellar lifetime of Maeder & Meynet (1989).

When a star dies, it enriches the ISM with its newly produced elements and with the unprocessed elements present in the star since its birth. Our model considers a detail pollution from SNe core-collapse ($M > 8$ $M_\odot$), AGB stars, NSMs, and SNe Ia, we follow the prescriptions for the single degenerate scenario of Matteucci & Greggio (1986). The iron yields for both SNe II and SNe Ia are the same as Cescutti et al. (2006).

In Fig. 1, we present graphically how the chemical enrichment proceeds in our stochastic model. For clarity, only 10 realizations are shown on the [Eu/Fe] versus [Fe/H] plane. The model has a constant delay time for NSM of 1 Myr and it is one of the models studied in Cescutti et al. (2015), namely NS00. In Fig. 1, we can appreciate how the time at which the first NSM explodes and pollute stars with europium, varies among the different realizations. Although the delay between the formation of NS binary and NSM is the same and very short, the formation of an NS binary is stochastic. So, we can have realizations where the first stars present europium after only ∼60 Myr, but also realizations where this happens later at around ∼130 Myr. A short formation delay implies less chemical enrichment of the volume. Therefore, the model results typically lie at high [Eu/Fe] and low [Fe/H], the contrary for longer delays (lower [Eu/Fe] and higher [Fe/H]).

In Fig. 1, the reader can also appreciate the different paths followed by each single realization in the [Eu/Fe] versus [Fe/H] plane. These paths show some patterns, which can be understood in terms of the enrichment that takes place in that region. For example, when a realization moves horizontally towards lower metallicities, there are no events enriching the ISM of iron or europium, and the gas is diluted by the infalling gas with primordial composition. Then, when an event produces Fe, the realization moves to higher metallicities and lower [Eu/Fe] ratios. If an NSMs explodes, the realization makes a jump towards higher [Eu/Fe] values. In general, the height of these 'jumps' varies for different realizations, due to the variable amount of Eu that a single NSM can produce (see equation 4).

3.1 Stellar yields for Eu

For the Eu production sites, we take into account both NSM and core-collapse SNe. We define three parameters to include the Eu production from NSM (Matteucci et al. 2014)

(i) the fraction of massive stars that generate a binary system of neutron stars that will eventually merge, $\alpha_{\rm NS}$.
(ii) the amount of Eu produced by a single merging event, $M^{\rm Eu}_{\rm NS}$.
(iii) the delay time between the formation of the binary system and the merging event. From now on we will call it coalescence time, $t_{\rm c}$.

In our work, we assume that a fixed fraction of massive stars, generated during the simulation, is the progenitor of NSMs. The progenitors are chosen randomly among all the generated massive stars in the mass range 8–50 $M_\odot$. We take the progenitor mass range as suggested in Matteucci et al. (2014). We assume a similar $\alpha_{\rm NS}$ to the one contained in Matteucci et al. (2014) (∼0.018), which is in agreement with the present-day neutron star merging rate of our Galaxy calculated by Kalogera et al. (2004) (∼80 Myr^{-1}).

For the nucleosynthesis of Eu, we use empirical values that have been chosen in order to reproduce the surface abundances of Eu in low-metallicity stars as well as the solar abundances of Eu (see Cescutti et al. 2006). These values are consistent with the limits calculated by Korobkin et al. (2012), who suggested that a single NSM can produce from 10^{-7} to 10^{-5} $M_\odot$ of Eu.

During the work, we have also considered a non-constant Eu production for a single NSM. In general, the variation is unknown, so we assume a range from 1 per cent of the average Eu ($M^{\rm Eu}_0$) to 200 per cent of it. Since the total mass of Eu produced should be preserved, the nth star ejects a mass of Eu that follows this equation:

$$M^{\rm Eu}_{\rm NS}(n) = M^{\rm Eu}_0(0.01 + 1.98 \cdot \mathrm{Rand}(n)) \quad (4)$$

where Rand(n) is a uniform random distribution in the rage [0,1] (same as in Cescutti & Chiappini 2014).

For the production of Eu from SNe II we adopt yields similar to those of Matteucci et al. (2014) (Mod2SNNS model). Since recent results showed that the conditions during an SN Type II explosion may not be able to produce much Eu (Arcones et al. 2007; Wanajo et al. 2011), we also tested an alternative channel: the MRD SNe. MRD SNe are a particular class of core-collapse SNe. Here, we assume that the 10 per cent of the CC-SNe explode as MRD. This r-process site is active only at low metallicity ($Z < 10^{-3}$), so it affects the model results only at low metallicity. These assumptions are identical to the ones contained in Cescutti et al. (2015). This particular fate is rare, only few SNe explode as MRD-SNe, and as mentioned in Winteler et al. (2012), it should be more likely to happen at low metallicity (Yoon, Langer & Norman 2006).

Downloaded from https://academic.oup.com/mnras/article/503/1/1/6127305 by inaf user on 05 August 2021

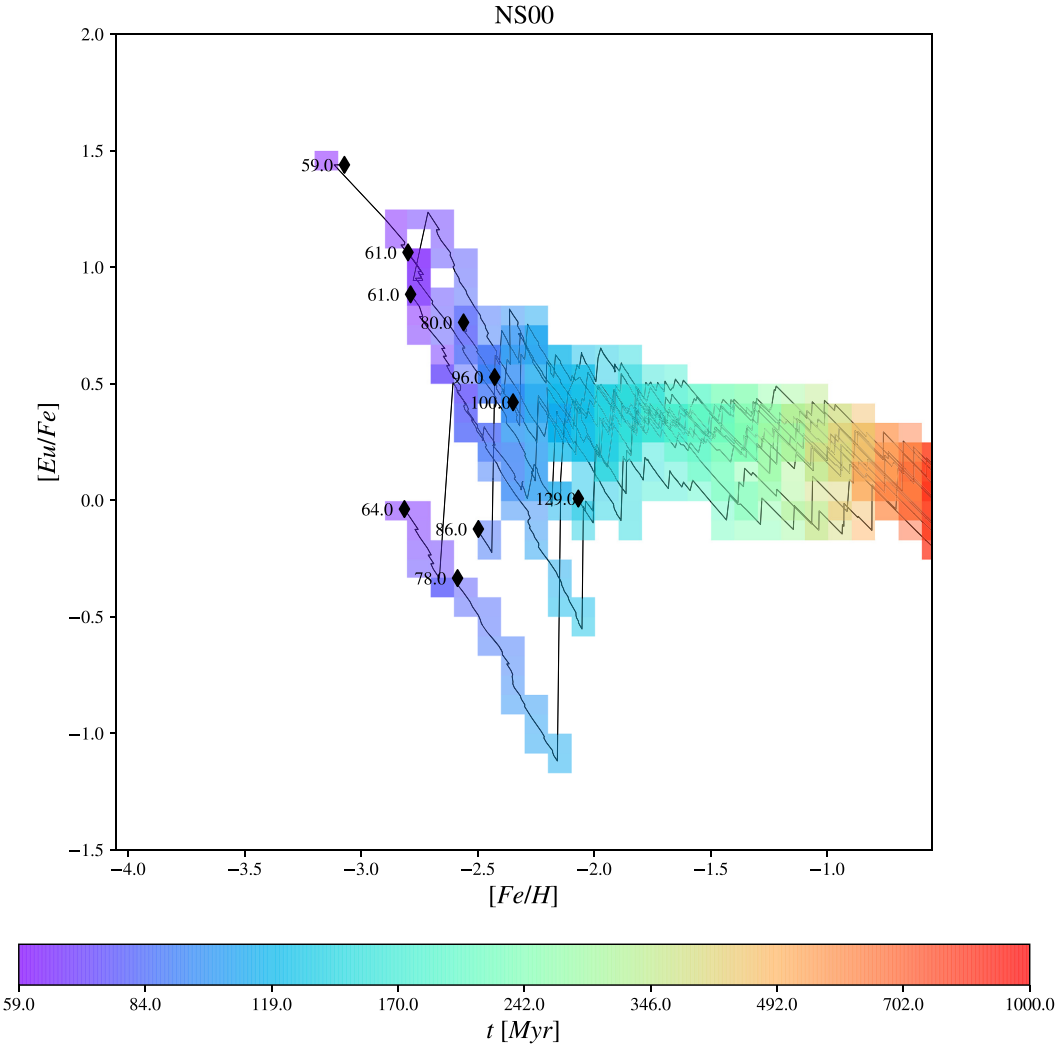

Figure 1. Results of [Eu/Fe] versus [Fe/H] for 10 realizations of NS00 model. As reported in Table 2, this model has a constant delay time for NSMs of 1 Myr. With the colour map, we show the time at which the realization pass through a certain point in the [Eu/Fe] versus [Fe/H] plane. We also report the initial point and the time at which the first NSM has exploded.

3.2 The coalescence time distribution for NSM

In this section, we present the different types of coalescence time-scale for NSM that we consider in our models. The DTD functions assumed in this work are $\propto t^{-1}$ and $\propto t^{-1.5}$ and defined as follows:

$$\mathrm{DTD}(t) = \begin{cases} 0 & \text{if } t < t^{\mathrm{c}}_{\mathrm{min}} \\ A_x t^{-x} & \text{if } t^{\mathrm{c}}_{\mathrm{min}} < t < 10\ \mathrm{Gyr} \\ 0 & \text{if } t > 10\ \mathrm{Gyr} \end{cases} \tag{5}$$

$$\text{with } x = \{1, 1.5\} \text{ and } A_x = 1/\int \tau^{-x} \mathrm{d}\tau;$$

where $t^{\mathrm{c}}_{\mathrm{min}}$ is the minimum coalescence time (in our models can assume two values: 1 and 10 Myr), and A_x is the normalization constant.

We also discuss possible tensions with observations.

3.2.1 Neutron star mergers with constant and short coalescence time-scale

As we mentioned in the Section 1, NSMs with a short and constant coalescence delay are able to reproduce the decreasing trend of [Eu/Fe] (also called knee) starting from [Fe/H] ~ -1 observed in the Galactic disc (Matteucci et al. 2014) and present also for α-elements. As showed by Cescutti et al. (2015), they can also explain the [Eu/Fe] spread in metal-poor stars in the Milky Way halo. However, a short and constant coalescence time is incompatible with several observations (see Côté et al. 2019; Simonetti et al. 2019). To begin with, if we assume that NSMs are progenitors of short-GRBs (Berger 2014), they cannot explain the observation of short GRBs in early-type galaxies, where star formation has stopped several Gyr ago. Furthermore, a short coalescence time-scale (<100 Myr) is inconsistent with the theoretical estimation of merging times of the seven known NS–NS binary systems, indeed their coalescence time-scale ranging from 86 to 2730 Myr (Tauris et al. 2017). Finally, as already mentioned, an NSM scenario with short and constant time-scales cannot explain the event GW170817 observed in an early-type galaxy.

Downloaded from https://academic.oup.com/mnras/article/503/1/1/6127305 by inaf user on 05 August 2021

Table 2. This table summarize the parameters of the models that we test during this work. It is organized as follows: in column 1, we report the name of the model, in column 2, the assumed DTD for coalescence time, in column 3, the minimum delay time for NSM, in column 4, the assumed fraction of massive star that could lead to NSM, in column 5, the assumed yield for NSM, in column 6, the assumed yield for MRD SNe. $^{\Psi}$ When we take into account the Eu production by MRD-SNe we set $\alpha_{\rm MRD} = 0.10$.

Model name	DTD	$t_{\rm c}^{\rm min}$ (Myr)	$\alpha_{\rm NS}$	$M_0^{\rm Eu;NSM}$ ($M_\odot$)	$M_0^{\rm Eu;MRD}$ ($M_\odot$)$^{\Psi}$
NS00	No	1	0.02	3×10^{-6} (varying as equation 4)	No production
NS01	”	10	”	”	”
NS02	”	100	”	”	”
NSt1	$\propto t^{-1}$	1	0.02	3×10^{-6} (varying as equation 4)	No production
NSt2	”	10	”	”	”
NSt3	$\propto t^{-1.5}$	1	”	3×10^{-6} (varying as equation 4)	”
NSt4	”	10	”	”	”
NS+MRD00	no	1	0.02	0.8×10^{-6} (varying as equation 4)	0.8×10^{-6} (varying as equation 4)
NS+MRD01	”	10	”	”	”
NS+MRD02	”	100	”	”	”
NS+MRDt1	$\propto t^{-1}$	1	0.02	0.8×10^{-6} (varying as equation 4)	0.8×10^{-6} (varying as equation 4)
NS+MRDt2	”	10	”	”	”
NS+MRDt3	$\propto t^{-1.5}$	1	”	”	”
NS+MRDt4	”	10	”	”	”
NSt3+α	$\propto t^{-1.5}$	1	Varying as equation 6 ($\overline{\alpha}_{\rm NS} = 0.275$)	3×10^{-6} (varying as equation 4)	No production
NSt1+α	$\propto t^{-1}$	1	”	”	”
Test1	$\propto t^{-1.5}$	1	Varying as equation 6 ($\overline{\alpha}_{\rm NS} = 0.275$)	3×10^{-6} (varying as equation 4)	No production
Test2	”	”	Varying as equation 6 ($\overline{\alpha}_{\rm NS} = 0.315$)	1.5×10^{-6} (varying as equation 4)	”
Test3	”	”	Varying as equation 6 ($\overline{\alpha}_{\rm NS} = 0.355$)	0.8×10^{-6} (varying as equation 4)	”

Table 1. Percentage of NSM already merged at different times for DTD of different shapes. Those values are for DTDs with a $t_{\rm c}^{\rm min} = 1$ Myr.

DTD	Per cent of NSMs exploded before		
	10 Myr	100 Myr	1000 Myr
$\propto t^{-1}$	25 per cent	50 per cent	75 per cent
$\propto t^{-1.5}$	69 per cent	91 per cent	98 per cent

3.2.2 *Neutron star mergers with a DTD* $\propto$ t^{-1}

In literature, a lot of authors have derived the DTD function of SNe Ia from observations. Most of the studies suggest that SNe Ia follow a DTD with the form $\propto t^{-1}$ (see Totani et al. 2008; Maoz & Badenes 2010; Graur et al. 2011; Maoz & Mannucci 2012; Rodney et al. 2014). This slope is also in agreement with predictions from population synthesis models. Similar techniques can be applied to derive the DTD of short-GRBs (i.e. the DTD of their progenitors: the NSMs).

Fong et al. (2017) found that, the DTD of short-GRBs can have the form of t^{-1}. A power law with a -1 slope is also in agreement with population synthesis studies (see Dominik et al. 2012; Chruslinska et al. 2018). Assuming a similar DTD for NSMs and SNe Ia (i.e. $\propto t^{-1}$) is also consistent with the fact that SNe Ia and short GRBs are detected in similar proportion in early-type galaxies. However, with this assumption on the DTD of NSMs, it was already shown that NSM cannot reproduce the decreasing trend of [Eu/Fe] in the Galactic disc (see Côté et al. 2019; Simonetti et al. 2019).

In our work, we tested this functional form for the DTD with three different lower bounds in the coalescence time: 1, 10, and 100 Myr. In order to include the coalescence time-scales of NS–NS systems contained in Tauris et al. (2017), we should have chosen an upper limit equal to ∞. In this work, we choose an upper limit of 10 Gyr because if we assume a larger one it would have changed only the normalization of the DTD, without a significant impact on the results.

3.2.3 *Neutron star mergers with a DTD* $\propto$ t$^{-1.5}$

We also tested a DTD $\propto t^{-1.5}$. This kind of slope is consistent with the distribution function of short-GRBs derived by D'Avanzo (2015). In particular, a steeper DTD function of the form of $t^{-1.5}$ is not in agreement with the fact that the observed fractions of short-GRBs and SNe Ia are similar. This disagreement could be eased if the DTD function of SNe Ia has also a $t^{-1.5}$ form, as suggested by Heringer et al. (2016), which showed that SNe Ia follow a DTD with a power-law slope in the range from -1.3 to -1.7. On the other hand, in the environment of a chemical evolution model, SNe Ia with a DTD $\propto t^{-1.5}$ are not able to reproduce all the [X/Fe] versus [Fe/H] trends in the Galaxy since, with a DTD $\propto t^{-1.5}$, the explosion time-scales of SNe Ia are too short (see Matteucci et al. 2006).

In the light of what we discuss in Section 3.2.2, this DTD is not in agreement with the one for SNe Ia and provides coalescence time-scales that are variable but still short. In fact, as shown in Table 1, more than 90 per cent of NSMs explode before 100 Myr.

4 RESULTS

In the following, we summarize the results of the models we computed, as shown in Table 2. They are distinguished in six classes. In the first class only NSM can produce Eu and is also assumed a constant coalescence time (NS0x). The second class of models test the effects of different DTDs on europium enrichment in the fist class scenarios (NStx). In the third class both NSM and MRD SNe are r-process sites. For NSM systems, we still assume a constant coalescence time. We also assume that, at metallicity ($Z < 10^{-3}$), 10 per cent of CC-SNe explode as an MRD (NS+MRD0x). In the fourth class, we test the effects of relaxing constancy of coalescence time in an NS + MRD scenario. We assume the same $\alpha = 0.1$ for MRD (NS+MRDtx). In the fifth class of models, we test a variable $\alpha_{\rm NS}$ versus [Fe/H] in an NS-only scenario (NStx+α). In the last class (Testx), we test the dependence between the value of $\alpha_{\rm NS}$ and the

Downloaded from https://academic.oup.com/mnras/article/503/1/1/6127305 by inaf user on 05 August 2021

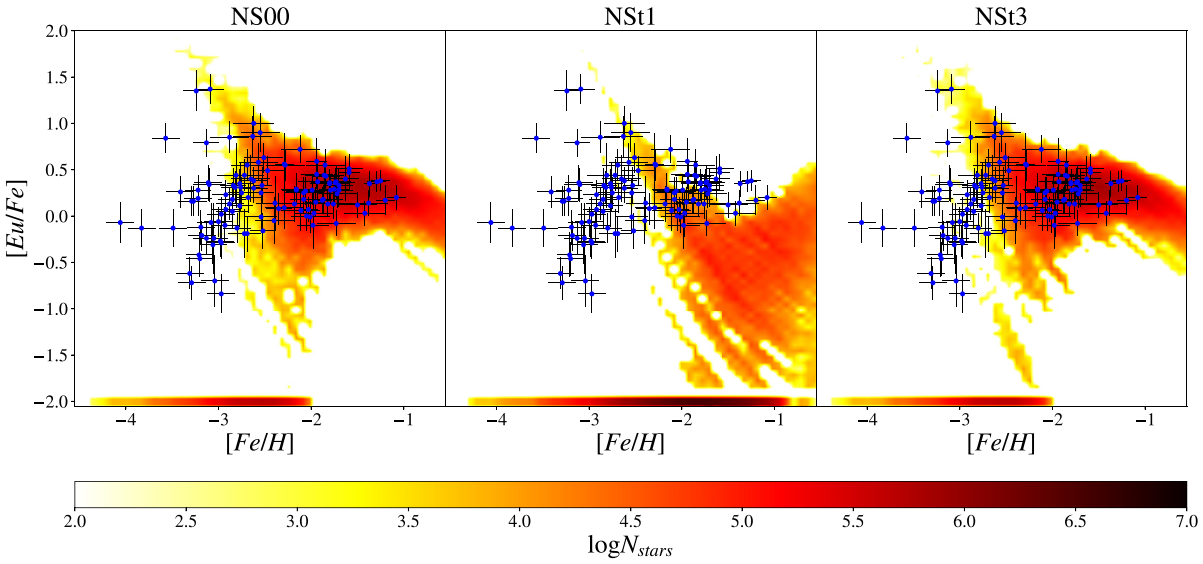

Figure 2. *Left-hand panel*: results of [Eu/Fe] versus [Fe/H] for model NS00. This model has a constant delay time for NSMs of 1 Myr, Eu production that vary as equation (4) and a mean value of 3×10^{-6} $M_{\odot}$, no Eu production from CC-SNe. Model NS00 is the same as NS00 contained in Cescutti et al. (2015). *Central panel*: same as *left-hand panel* but for model NSt1. The only difference from the previous model is the assumption on the coalescence time; in fact in this case we assume a delay time with a DTD $\propto t^{-1}$ for NSMs. *Right-hand panel*: same as previous panels but for model NSt3. In this model for the coalescence time of NSMs we assume a DTD $\propto t^{-1.5}$. Note that all the models contained in this figure has minimum coalescence time set to 1 Myr. The long-living stars formed without Eu (formally [Eu/Fe] $= -\infty$) are shown at [Eu/Fe] $= -2.0$ dex.

dispersion of the results at moderate metallicity (~ -1.5 dex). In Figs 2-7 are shown the results, in the [Eu/Fe] versus [Fe/H] plane, from our models. In the plots, at [Eu/Fe] $= -2.0$ dex, we also report the long-living stars formed without Eu (formally [Eu/Fe] $= -\infty$).

4.1 Models with only NSM

In Fig. 2 is shown the distribution of the long-living stars in the [Eu/Fe]–[Fe/H] plane, as predicted by our stochastic models with the following assumptions: (i) Eu is produced only from NSM whose progenitors are in the mass range from 9 to 50 $M_{\odot}$. (ii) The amount of Eu produced from a single event follows equation (4) with an average value ($M_0^{\rm Eu}$) of 3×10^{-6} $M_{\odot}$. (iii) 2 per cent of massive stars are in binary systems with the right characteristics to lead to NSM. (iv) The minimum value for the coalescence time is fixed at 1 Myr. The plotted models are NS00, NSt1, and NSt3 (cf. Table 2). In the left-hand panel of Fig. 2 is seen that the NS00 model is in agreement with the data for stars with [Fe/H] > -3 but it cannot explain the presence of stars with [Eu/Fe] < 0 for [Fe/H] < -3. Finally, the model does not predict stars with [Eu/Fe] < -0.1 at [Fe/H] < -3.

The reasons of the peculiar diagonal shape in the model results from high [Eu/Fe] with low [Fe/H] to low [Eu/Fe] with higher [Fe/H] (described in Cescutti et al. 2015) are the following: the upturn in [Eu/Fe], visible at low metallicities, is a consequence of the fixed amount of Eu produced by NSM, coupled with the paucity of NSM events and the constant mixing volume assumed in our model. When an NSM pollutes a simulated box early on, it produces a value in the [Eu/Fe] versus [Fe/H] space, dependent on the mass of the previous enriching SNe II. The volume enriched by NSM and SNe II with the lowest amount of iron creates the upper tip of this upturn towards low metallicity. Then in all the volumes polluted by NSM, the probability of having another Eu enrichment is low, so they evolve towards lower [Eu/Fe] and higher [Fe/H] by the subsequent enrichment of Fe by SNe II, creating the diagonal shape from high [Eu/Fe] with low [Fe/H] to low [Eu/Fe] with higher [Fe/H]. Indeed, the model struggles to reproduce the stars with [Eu/Fe] < 0 dex at the lowest metallicities. We will examine in details this problem in a future work.

When we drop the constancy of the coalescence time and we use a DTD $\propto t^{-1}$ the situation is even worse. In the model, NSt1 (middle panel) fails to reproduce the distribution of the observational data. Finally, when we take into account a DTD $\propto t^{-1.5}$ (NSt3), we obtain similar results of NS00 model. In fact, as shown in Fig. 2 (right-hand panel), the model cannot explain the presence of stars with [Eu/Fe] < -0.4 at [Fe/H] < -2.8. NSt3 also predicts stars with [Eu/Fe] < -0.2 in the metallicity range $-2.0 <$ [Fe/H] < -1.0. We should notice that results from NS00 and NSt3 are similar. This is due to the fact that a power law with a -1.5 slope keeps the coalescence times short even if they are not constant as mentioned in Section 3.2.3).

The situation does not change if we assume a minimum coalescence time of 10 Myr (Fig. 3). In Fig. 3, we show the results by models with the following assumptions: (i) Eu is produced only from NSM and their progenitors are in the mass range from 9 to 50 $M_{\odot}$. (ii) The amount of Eu produced from a single event follows equation (4) with an average value ($M_0^{\rm Eu}$) of 3×10^{-6} $M_{\odot}$. (iii) 2 per cent of massive stars are in binary systems with the right characteristics to lead to merging NS. (iv) The minimum value for the coalescence time is fixed at 10 Myr. The plotted models are NS02, NSt2, and NSt4 (see Table 2). In the left-hand panel of Fig. 3, we can notice that the model NS01 does not predict the presence of stars with [Eu/Fe] $<$ 0.3 dex for metallicity lower than -2.8 dex. On the other hand, there is good agreement with the observed europium abundances of stars with [Fe/H] > -2.7 dex.

For model NSt2 (central panel of Fig. 3), the situation is similar to model NSt1 (central panel of Fig. 3). Again, when we drop the constancy of the coalescence time and we also assume a DTD $\propto t^{-1}$, models completely fail to reproduce the observational data. Finally, model NSt4, which assumes a DTD $\propto t^{-1.5}$, fails to reproduce europium abundances of stars with [Fe/H] < -2.8 dex. With a

Downloaded from https://academic.oup.com/mnras/article/503/1/1/6127305 by inaf user on 05 August 2021

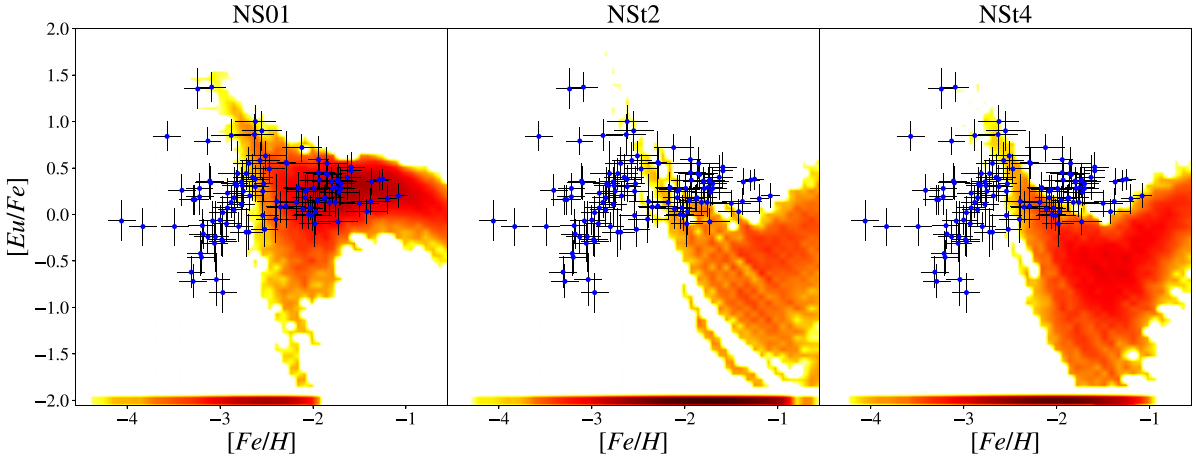

Figure 3. *Left-hand panel*: results of [Eu/Fe] versus [Fe/H] for model NS01. This model has a constant delay time for NSMs of 10 Myr, Eu production that vary as equation (4) and a mean value of 3×10^{-6} M$_\odot$, no Eu production from CC-SNe. Model NS01 is the same as NS01 contained in Cescutti et al. (2015).*Central panel*: same as *left-hand panel* but for model NSt2. The only difference from the previous model is the assumption on the coalescence time; in fact in this case we assume a delay time with a DTD $\propto t^{-1}$ for NSMs. *Right-hand panel*: same as previous panels but for model NSt4. In this model for the coalescence time of NSMs we assume a DTD $\propto t^{-1.5}$. Note that all the models contained in this figure has minimum coalescence time set to 10 Myr.

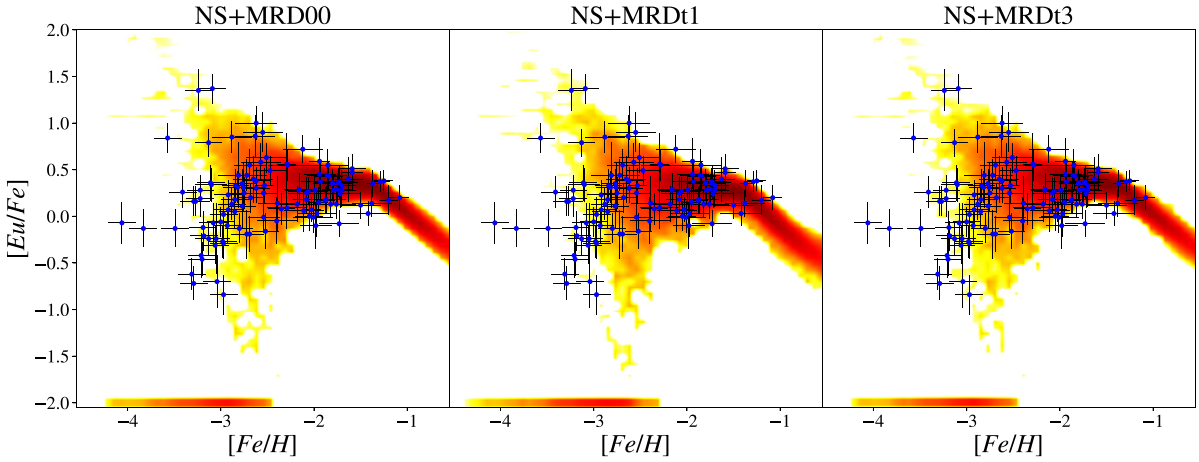

Figure 4. *Left-hand panel*: results of [Eu/Fe] versus [Fe/H] for model NS + MRD00. This model has a constant delay time for NSMs of 1 Myr, Eu production from NSMs that varying as equation (4) and a mean value of 0.8×10^{-6} M$_\odot$, Eu production from MRD-SNe (10 per cent of CC-SNe only at $Z < 10^{-3}$) that vary as equation (4) and a mean value of 0.8×10^{-6} M$_\odot$. *Central panel*: same as *left-hand panel* but for model NS + MRDt1. The only difference from the previous model is the assumption on the coalescence time; in fact in this case we assume a delay time with a DTD $\propto t^{-1}$ for NSMs with. *Right-hand panel*: same as previous panels but for model NS + MRDt3. In this model for the coalescence time of NSMs we assume a DTD $\propto t^{-1.5}$. Note that all the models contained in this figure have minimum coalescence time set to 1 Myr.

mean value of 3×10^{-6} M$_\odot$ for the Eu production, it also cannot reproduce some stars of the upper envelope of the observed star distribution.

4.2 Models with NSM and MRD-SNe

As seen in the previous section, a scenario, where NSMs are the only r-process site, fails to predict the presence of Eu in stars with metallicity [Fe/H] < -2.8 dex, even if we assume a constant and short delay time with our stochastic model. A scenario where CC-SNe are the only r-process site is not supported by nucleosynthesis models (see Arcones et al. 2007; Arcones & Thielemann 2012): in particular, neutrino winds in SNe II explosions are proton-rich and therefore they struggle to produce the heaviest neutron-capture elements (such as Eu). On the other hand, Siegel, Barnes & Metzger (2019) noticed that collapsar (collapse of rotating massive stars) accretion discs also produce neutron-rich outflows that synthesize heavy r-process nuclei, despite the comparatively proton-rich composition of the infalling star. In Section 3.1, we discussed an alternative channel for the Eu production: the MRD SNe. Now, we want to test if a scenario where both NSMs and MRD-SNe can produce Eu is able to reproduce the abundance of Eu the halo stars.

In Fig. 4, we report the results of our models with the following assumptions: (i) Eu is produced both from NSMs and MRD-SNe. (ii) the progenitors of NSMs are in the mass range from 9 to 50 M$_\odot$. (ii) The amount of Eu produced from a single NSM event follows equation (4) with an average value $M_0^{\rm Eu;NSM} = 0.8 \times 10^{-6}$ M$_\odot$. (v)

Downloaded from https://academic.oup.com/mnras/article/503/1/1/6127305 by inaf user on 05 August 2021

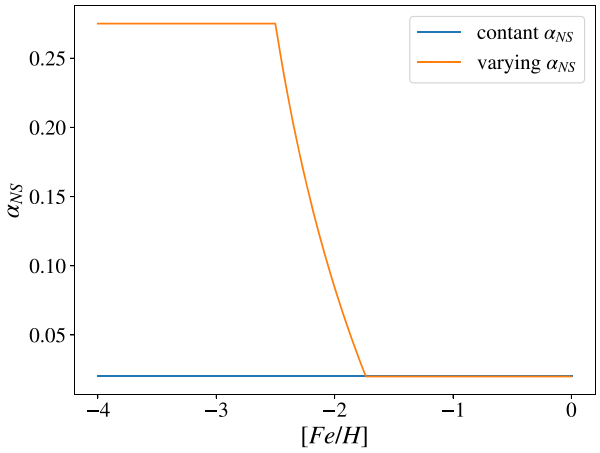

Figure 5. The evolution with metallicity of $\alpha_{\rm NS}$ in two different scenarios.

2 per cent of massive stars are in binary systems with the right characteristics to lead to merging NS. (iv) At low metallicity ($Z < 10^{-3}$), 10 per cent of CC-SNe explode as MRD. (v) the amount of Eu produced by a single MRD explosion follows equation (4) with an average value $M_0^{\rm Eu;MRD} = 0.8 \times 10^{-6}$ M$_\odot$ (same as NSMs). The plotted models are NS+MRD00, NS+MRDt1, and NS+MRDt3 (cfr. Table 2).

Model NS+MRD00 (right-hand panel of Fig. 4) is in good agreement with the observational data and it well predicts the presence of stars with [Fe/H] < -3 dex and [Eu/Fe] < 0 dex. Moreover, also assuming the two different DTDs for NSM, we can still reproduce the data, see Fig. 4 middle and right-hand panels. This is not surprising, since the model at low metallicity, in this case, is basically enriched by MRD SNe. It has been shown also in Cescutti et al. (2015); in that paper they used a delay for NSM of 100 Myr, $\alpha_{\rm NS} = 0.02$, every NSM producing a constant amount of Eu equal to 1.5×10^{-6} M$_\odot$ and a single MRD SN produces, on average, 1×10^{-6} M$_\odot$ and 10 per cent of stars in the mass range 8–80 M$_\odot$ explodes as MRD SNe.

4.3 Models with variable $\alpha_{\rm NS}$

Another possible way to solve it is to relax the assumption of constancy of the fraction of massive stars that can generate a binary system of neutron stars which will eventually merge, $\alpha_{\rm NS}$.

Several works investigate the formation of double NS systems (Bogomazov, Lipunov & Tutukov 2007; Ivanova et al. 2008; Mennekens & Vanbeveren 2014; Shao & Li 2018). In particular, as shown in Giacobbo & Mapelli (2018), metallicity plays a crucial role in the formation of binary systems of compact objects. For these reasons, we decide to test this scenario with our chemical evolution model.

We assume a dependence of $\alpha_{\rm NS}$ on [Fe/H] (see Fig. 5) similar to the one assumed in model 4AV2 contained in Simonetti et al. (2019). With this assumption $\alpha_{\rm NS}$ varies as

$$\alpha_{\rm NS}([{\rm Fe/H}]) = \begin{cases} \overline{\alpha}_{\rm NS} & \text{if } [{\rm Fe/H}] \leq -2.5 \\ \overline{\alpha}_{\rm NS}(1 - ln([{\rm Fe/H}] + z_0) + z_1) & \text{if } [{\rm Fe/H}] > -2.5 \\ \alpha_{\rm NS}^{\rm min} & \text{if } \alpha_{\rm NS} < \alpha_{\rm NS}^{\rm min} \\ z_0 = 3.0\,{\rm dex}; z_1 = ln(0.5) & \end{cases} \quad (6)$$

In order to test this scenario we have built a new model (NSt3+α) with the following assumptions: (i) Eu is produced only from NSM, whose progenitors are in the mass range from 9 to 50 M$_\odot$. (ii) The amount of Eu produced from a single event follows equation (4) with an average value ($M_0^{\rm Eu}$) of 3×10^{-6} M$_\odot$. (iii) The parameter $\alpha_{\rm NS}$ depends on [Fe/H] and varying as equation (6); $\overline{\alpha}_{\rm NS}$ is set to 0.275. (iv) The coalescence time distribution of NSMs follows a DTD $\propto t^{-1.5}$. This system has a minimum delay time of 1 Myr. The predictions of NSt3+α are plotted in left-hand panel of Fig. 6. It is seen that this model is in good agreement with the observational data, but it is not able to predict the presence of stars with low [Eu/Fe] (<-0.5) at [Fe/H] < -3.0. NSt3+α model predicts also the presence of stars with [Eu/Fe] < -0.5 even at relative high metallicity ([Fe/H] > -2.0) that cannot be confirmed by the chosen data sample. Last, as seen in all the tested models of this work, the model cannot explain the presence of Eu in stars with [Fe/H] < -3.5 dex.

Then, we tested a model with $\alpha_{\rm NS}$ variable and the DTD $\propto t^{-1}$. We built NSt1+α model with the following assumptions: (i) Eu is produced only from NSM, whose progenitors are in the mass range from 9 to 50 M$_\odot$. (ii) The amount of Eu produced from a single event follows equation (4) with an average value ($M_0^{\rm Eu}$) of 4×10^{-6} M$_\odot$. (iii) The parameter $\alpha_{\rm NS}$ depends on [Fe/H] and varies as equation (6); $\overline{\alpha}_{\rm NS}$ is set to 0.275. (iv) The coalescence time of NSMs follows a DTD $\propto t^{-1}$ and has a minimum value of 1 Myr. The results of this model are shown in the right-hand panel of Fig. 6. As you can notice, the model does not predict the presence of stars with [Eu/Fe] < 0.3 at metallicity lower than -2.9 dex. On the other hand, the model shows good compatibility with the upper envelope of the stars' abundance distribution. We should also notice that in the region with [Eu/Fe] < -0.4 at metallicity larger than -2.5 dex, there is a strong excess in the predicted star distribution that is not supported by observational data.

By a simple comparison between the right-hand panel of Fig. 6 and central panel of Fig. 2 we can assert that dropping the constancy of $\alpha_{\rm NS}$ as a function of [Fe/H] has a great impact on the results of our chemical evolution models. In particular, an $\alpha_{\rm NS}$ that varies with metallicity, can substitute MRD-SNe in the framework of explaining the low-Eu tail of metal-poor halo stars ([Fe/H] < -2.5 dex).

4.4 Test on the dispersion at intermediate metallicity

In this section, we explore the correlation between the dispersion of the [Eu/Fe] values and the fraction of massive stars that can produce an NSM, namely the parameter $\alpha_{\rm NS}$.

We start from the assumptions of our best model (NSt3+α) and then we increase the value of $\alpha_{\rm NS}$. With these prescriptions we create three different models (see Table 2): (i) Test1 is exactly the same as NSt3+α. (ii) Test2; for this model, we assume $\overline{\alpha}_{\rm NS}= 0.315$ (see equation 6). This implies a slight increase of NSMs at the lowest metallicities, but it also implies an increase of a factor of 3 at [Fe/H] > -1.5. Due to this variation, the total number of NSM is increased by a factor $\sim$2.5. For this reason, since we want to keep approximately constant the total amount of Eu, we have to decrease $M_0^{\rm Eu;NSM}$ to 1.5×10^{-6} M$_\odot$. (iii) Test3; in this case we set $\overline{\alpha}_{\rm NS}= 0.375$. As a consequence of this, the total number of NSM is increased by a factor $\sim$5. Also, in this case, we reduce the mean Eu produced to 0.8×10^{-6} M$_\odot$.

On the results of these models, we select different bins in metallicity and in these we compute mean and standard deviation of [Eu/Fe] values. The mean and standard deviation for each model

Downloaded from https://academic.oup.com/mnras/article/503/1/1/6127305 by inaf user on 05 August 2021

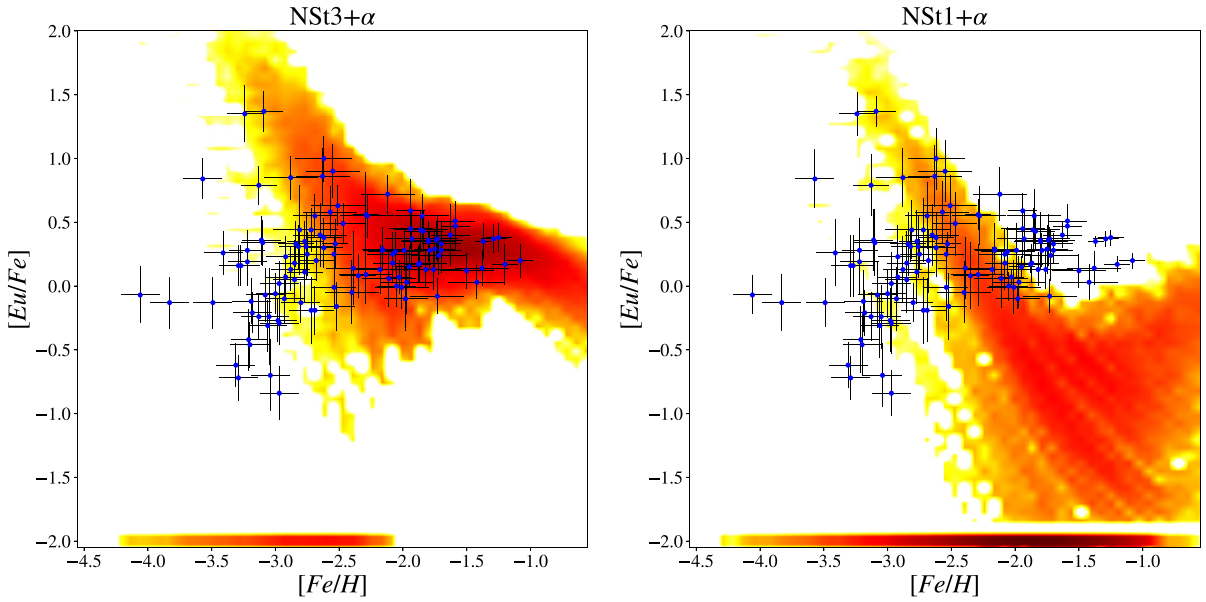

Figure 6. *Left-hand panel*: results of [Eu/Fe] versus [Fe/H] for model NSt3+α. Comparing this panel with the right one of Fig. 2 is clear that a variable α_I has a great impact on the stars distribution predicted by our models. In particular, an $\alpha_{\rm NS}$ that depends on the metallicity allows models to generate stars Eu-enriched at lower metallicity. *Right-hand panel*: same as *left-hand panel* but for model NSt1+α. In this case a variable $\alpha_{\rm NS}$ has the same effect and improves the compatibility between model results and observational data in the metallicity range $-2.8 <$ [Fe/H] < -2.5.

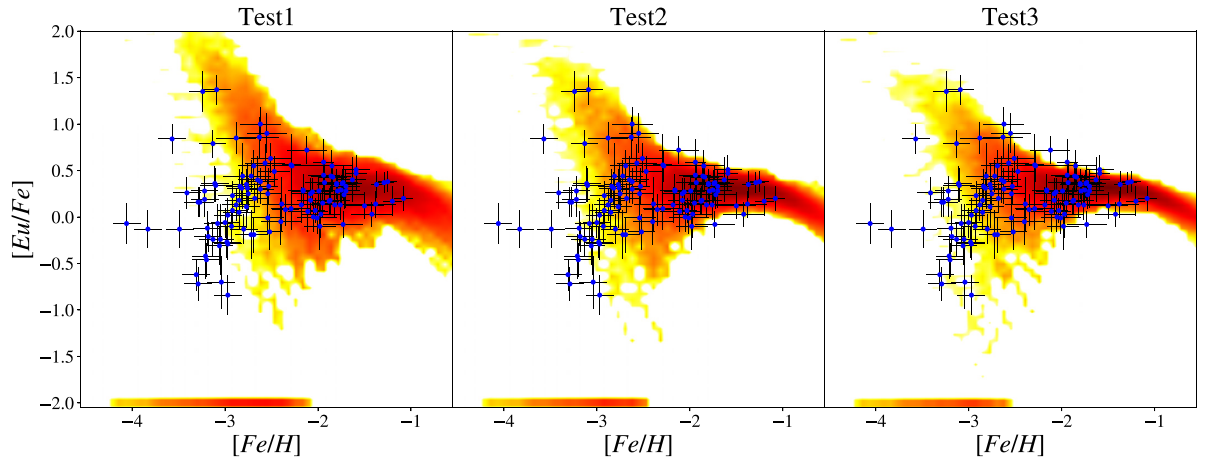

Figure 7. *Left-hand panel*: results of [Eu/Fe] versus [Fe/H] for model Test1. This model is identical to NSt3+α model. We plot it again to emphasize the consequences of the variation of $\alpha_{\rm NS}$ and $M_0^{\rm Eu}$. *Central panel*: same as *left-hand panel* but for model Test2. In this model, the equation (6) is up-shifted by 0.04, the function shows two plateau with $\alpha_{\rm NS} = 0.315$ and 0.06. In order to maintain constant the total amount of produced Eu, we reduce $M_0^{\rm Eu}$ to 1.5×10^{-6} $M_\odot$. *Right-hand panel*: same as *left-hand panel* but for model Test3. This model, the $\alpha_{\rm NS}$ versus [Fe/H] relation, is up-shifted by 0.08 therefore the function, described by equation 6, shows two plateau with $\alpha_{\rm NS} = 0.355$ and 0.1. In this case $M_0^{\rm Eu}$ is reduced to 0.8×10^{-6} $M_\odot$.

are reported in Table 3. In Fig. 7 are plotted the results of the three models: Test1, Test2, and Test3.

Looking at Fig. 7, focusing at the region at the intermediate metallicity, it can be easily noticed that the observational data cannot exclude any of the tested models. Indeed, stochastic models with a large variation of $\alpha_{\rm NS}$ (from 0.02 to 0.10) predict differently the enrichment at intermediate metallicity regime. On the other hand, the observational data are affected by relatively large uncertainties (i.e. ~0.2–0.3 dex in [Eu/Fe]); moreover, the sample selected is certainly measured in a homogeneous way, but it is not large enough to apply safely a statistical approach. Adding more authors will increase the number of data, but we risk to increase significantly the scatter among different authors. Future surveys such as 4MOST (de Jong et al. 2014) and WEAVE (Dalton et al. 2012) will surely produce larger data set homogeneously measured and they could allow us to determine the value of $\alpha_{\rm NS}$, and consequently $M_0^{\rm Eu;NSM}$, more precisely.

Downloaded from https://academic.oup.com/mnras/article/503/1/1/6127305 by inaf user on 05 August 2021

Table 3. Here are summarized the results of our analysis. The table is organized as follows: in column 1, the metallicity value to which we compute mean and standard deviation of the [Eu/Fe] values, in column 2, mean [Eu/Fe] at some metallicity for a specific model, in column 3, the standard deviation at some metallicity for a specific model, in column 4, fraction of Eu-free ($f = N_{\text{Eu-free}}/N_{\text{tot}}$). This structure is repeated for the three different models contained in this section.

[Fe/H] (dex)	Test1			Test2			Test3		
	Mean [Eu/Fe] (dex)	Sigma (dex)	f	Mean [Eu/Fe] (dex)	Sigma (dex)	f	Mean [Eu/Fe] (dex)	Sigma	f
−3.00	1.11	0.32	0.34	0.76	0.31	0.26	0.62	0.26	0.20
−2.75	0.89	0.27	0.21	0.59	0.25	0.11	0.50	0.20	0.05
−2.50	0.61	0.24	0.11	0.44	0.19	0.05	0.40	0.15	0.02
−2.25	0.44	0.19	0.02	0.36	0.15	0.00	0.34	0.11	0.00
−2.00	0.36	0.16	0.01	0.33	0.11	0.00	0.33	0.08	0.00
−1.75	0.33	0.13	0.00	0.32	0.09	0.00	0.31	0.07	0.00
−1.50	0.31	0.11	0.00	0.31	0.07	0.00	0.31	0.06	0.00
−1.25	0.31	0.10	0.00	0.31	0.06	0.00	0.30	0.05	0.00
−1.00	0.27	0.10	0.00	0.27	0.06	0.00	0.27	0.05	0.00

4.4.1 *Eu-free stars*

All the tested models have a common feature: the considered r-process events are rare and they are only a small fraction (α_{NS}) of the total number of the main polluters of the ISM at low metallicity, the SNe II. It is easy to infer that, at extremely low metallicities ([Fe/H] ≤ -3), a lot of low-mass stars can be formed in regions where the ISM is not yet polluted by r-process events. We also expect that lowering the fraction α_{NS} should lead to an increase of Eu-free stars (i.e. [Eu/Fe] $= -\infty$). Moreover, a longer time delay for the r-process events will also produce a higher fraction of Eu-free stars, since for a longer time ISM will be not enriched by r-process events.

All the plots of our models (Fig. 2–7) show the long-living stars formed without Eu (i.e. Eu-free stars) at [Eu/Fe] $= -2.0$ dex. From these plots, it is possible already to find a behaviour that is in agreement with our aforementioned expectations. For example, looking at Fig. 2, is possible to notice that a model with a DTD function with the form $\propto t^{-1}$ (NSt1) predicts a higher number of Eu-free star compared to both the short and constant delay presented NS00 and the steeper DTD ($\propto t^{-1.5}$) of NSt3 models.

However, to better study the behaviour of the Eu-free stars with respect to the fraction α_{NS}, we report in Fig. 8, the ratio of Eu-free stars over the total number of stars for the models Test1, Test2, and Test3. In this plot, it appears clearly that increasing α_{NS}, so moving from Test1 to Test3, the model predicts a lower fraction of Eu-free stars. Observationally, it is not obvious how to put constraints to the modelling since no Eu-free star has been yet claimed. On the other hand, several stars have only upper limits for europium. In Fig. 8, we decide to use as a proxy of Eu-free stars, stars for which only upper limits for europium have been detected and barium is measured, as already assumed in Cescutti et al. (2015). In the plot, we use two data set to compute this observational proxy. So together with the results obtained with the stars measured in Roederer et al. (2014), we show also the results obtained in Cescutti et al. (2015) adopting a different data set. Details of this collection can be found in Cescutti et al. (2015). We decide to add these results, because it appears clear that the number of upper limits detected by Roederer et al. (2014) for europium are quite high and possibly due to a certain fraction of spectra missing the necessary quality to measure europium, rather than the real absence of this element. So, we trust more the results from the larger sample used in Cescutti et al. (2015) towards higher metallicity, whereas for low metallicity, they appear in reasonable agreement. In comparison, our models predictions appear to follow the trend, but it is always below the observational proxy. This can be explained by a large fraction of false Eu-free stars, due to the difficulty of measuring the weak europium lines when the abundance is really low. Overall, our best model (i.e. Test 1) appears in agreement with this observational proxy, but it is hard to find a firm conclusion from this prospective.

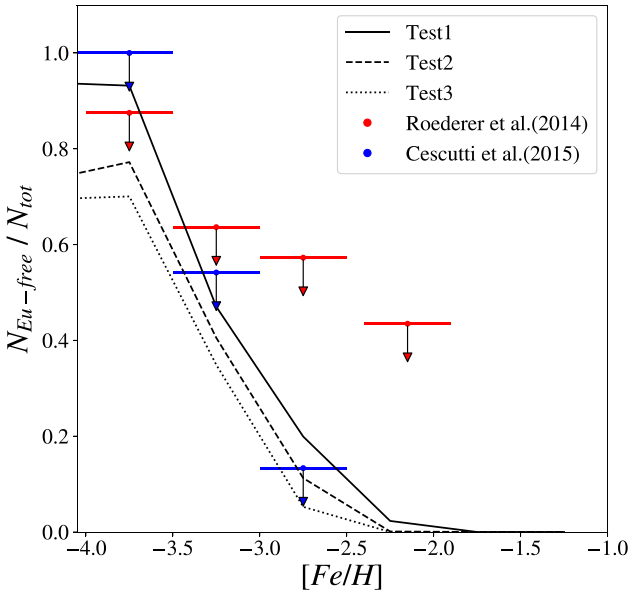

Figure 8. Ratio of Eu-free stars over the total number of stars for bins of 0.5 dex in [Fe/H]. In the figure are plotted the results for the models Test1, Test2, and Test3. The blue triangles are the observational proxy for this ratio, so the ratio between the number of stars in which Eu only presents an upper limit (possibly Eu-free) over the number of stars for which at least Ba has been measured (total number of stars). The horizontal error bars show the dimension of each bin in [Fe/H]. Red triangles are the observational proxy for this ratio derived from the data set used in this work (Roederer et al. 2014). The blue triangles are the same observational proxy calculated in Cescutti et al. (2015); adopting a different data set (cfr. Cescutti et al. 2015, for details on this data set).

5 CONCLUSIONS

In this paper, we have adopted the stochastic chemical evolution model of the Galactic halo presented by Cescutti (2008), to study the impact of relaxing the constancy of the delay times for the coalescence of NSM, on the chemical evolution of Eu in the metal-poor environment of the Galactic halo. To perform that, we have

Downloaded from https://academic.oup.com/mnras/article/503/1/1/6127305 by inaf user on 05 August 2021

implemented two different DTDs $\propto t^{-1}$ and $\propto t^{-1.5}$, as suggested in Côté et al. (2019). For the Eu yields, we have followed the prescriptions of Matteucci et al. (2014) and Cescutti et al. (2015). We have also tried to find a way to solve the tensions between the observational data and the results of models that assume a variable coalescence time. In order to do that, we have explored a scenario in which both NSM and MRD SNe are able to produce Eu. For the same reason, we have also implemented a fraction of massive stars that can produce NSM systems that vary with metallicity, following the idea presented in Simonetti et al. (2019). Finally, we have also studied the [Eu/Fe] versus [Fe/H] in the Galactic halo and its correlation with the value of $\alpha_{\rm NS}$.

Our main conclusions can be summarized as follows:

(a) The NS-only scenario is in disagreement with observational data, even at moderate metallicity, when we assume a DTD $\propto t^{-1}$ for the coalescence time-scales. On the other hand, assuming a DTD $\propto t^{-1.5}$ produces results similar to the ones with constant delay time. These conclusions are similar to the ones found by Côté et al. (2019), but now we obtain these results in the framework of a stochastic chemical evolution model.

(b) The mixed scenario with NS and MRD SNe is able to explain the observed spread as shown, but only for a constant delay, in Cescutti et al. (2015). The main assumptions, in this case, are that MRD SNe are 10 per cent of CC-SNe, explode only at low metallicity ($Z < 10^{-3}$) and the production of Eu is the same for both NSM and MRD SNe. We prove here that the models in this case agree with observations independently by the assumed DTD.

(c) Our best NS-only scenario is in good agreement with observational data under the following assumptions: (i) Eu is produced only from NSM, whose progenitors are in the mass range from 9 to 50 $M_{\odot}$. (ii) The amount of Eu produced from a single event follows equation (4) with an average value ($M_0^{\rm Eu}$) of 3×10^{-6} $M_{\odot}$. (iii) The parameter $\alpha_{\rm NS}$ depends on [Fe/H] and varies as equation (6); the required $\overline{\alpha}_{\rm NS}$ is 0.275. (iv) The coalescence time distribution of NSMs should follow a DTD $\propto t^{-1.5}$ with a minimum value of 1 Myr. In this scenario, a larger fraction of NSM explodes in the early phases of the Galactic evolution, compared to nowadays (see also Simonetti et al. 2019).

(d) Adopting to our best model, we also show the predicted dispersion of [Eu/Fe] at a given metallicity depending on the equation (6); the comparison with the present literature data cannot allow us to put a stronger constraint (6). However, future high-resolution spectroscopical surveys, such as 4MOST (de Jong et al. 2014) and WEAVE, (Dalton et al. 2012) will produce the necessary statistic to constrain at best this parameter.

(e) Our best model is in agreement with the chosen observational proxy for Eu-free stars. However, the fraction of false Eu free stars cannot be evaluated and no firm conclusions can be raised.

The models struggle to reproduce the low-metallicity tail of stars with [Eu/Fe] < -0.1 dex at [Fe/H] < -3.0 dex. We underline that the model at this stage does not consider several complexities that can play an important role to solve this issue, for example: stochasticity in SFR and infall-law, cross-contamination of sub-haloes, pre-enrichment of the infalling gas, and multiphase ISM.

In future work, we will try to solve this problem by taking into account the hierarchical formation of Galactic halo by accretion of satellite galaxies. In fact, the enrichment of r-process elements in these objects could have been less effective due to dynamical effects connected to the formation of binary neutron stars (see Bonetti et al. 2019).

ACKNOWLEDGEMENTS

We thank the referee for comments that improved the quality of this paper. We also thank Paolo Simonetti for assistance with the implementation of the time delay distributions. This work has been partially supported by the European Union Cooperation in Science and Technology (COST) Action CA16117 (ChETEC). GC acknowledges funding from the Istituto Nazionale di Astrofisica (INAF) mainstream 2018 program 'The origin of lithium: a key element in astronomy'.

DATA AVAILABILITY

The data underlying this article will be shared on reasonable request to the corresponding author.

REFERENCES

Abbott B. P. et al., 2017a, Phys. Rev. D, 95, 082005
Abbott B. P. et al., 2017b, Phys. Rev. Lett., 119, 161101
Abohalima A., Frebel A., 2018, ApJS, 238, 36
Arcones A., Thielemann F.-K., 2012, J. Phys. G: Nucl. Part. Phys., 40, 013201
Arcones A., Janka H.-T., Scheck L., 2007, A&A, 467, 1227
Argast D., Samland M., Thielemann F.-K., Qian Y.-Z., 2004, A&A, 416, 997
Bauswein A., Goriely S., Janka H. T., 2013, ApJ, 773, 78
Berger E., 2014, Ann. Rev. Astron. Astrophys., 52, 43
Bisterzo S. et al., 2015, MNRAS, 449, 506
Bogomazov A., Lipunov V., Tutukov A., 2007, Astron. Rep., 51, 308
Bonetti M., Perego A., Dotti M., Cescutti G., 2019, MNRAS, 490, 296
Cameron A., , 1982, Essays in Nuclear Astrophysics, Cambridge: University Press, Cambridge. p. 23,
Cescutti G., 2008, A&A, 481, 691
Cescutti G., Chiappini C., 2014, A&A, 565, A51
Cescutti G., François P., Matteucci F., Cayrel R., Spite M., 2006, A&A, 448, 557
Cescutti G., Romano D., Matteucci F., Chiappini C., Hirschi R., 2015, A&A, 577, A139
Chiappini C., Ekström S., Meynet G., Hirschi R., Maeder A., Charbonnel C., 2008, A&A, 479, L9
Chruslinska M., Belczynski K., Klencki J., Benacquista M., 2018, MNRAS, 474, 2937
Côté B. et al., 2019, ApJ, 875, 106
Coulter D. et al., 2017, Science, 358, 1556
Cowan J. J., Thielemann F.-K., Truran J. W., 1991, Phys. Rep., 208, 267
D'Avanzo P., 2015, J. High Energy Astrophys., 7, 73
Dalton G. et al., 2012, in McLean I. S., Ramsay S. K., Takami H., eds, Proc. SPIE Conf. Ser. Vol. 8446, Ground-based and Airborne Instrumentation for Astronomy IV. SPIE, Bellingham, p. 84460P
de Jong R. S. et al., 2014, in Ramsay S. K., McLean I. S., Takami H., eds, Proc. SPIE Conf. Ser. Vol. 9147, Ground-based and Airborne Instrumentation for Astronomy V. SPIE, Bellingham, p. 91470M
Dominik M., Belczynski K., Fryer C., Holz D. E., Berti E., Bulik T., Mandel I., O'Shaughnessy R., 2012, ApJ, 759, 52
Eichler D., Livio M., Piran T., Schramm D. N., 1989, Nature, 340, 126
Fong W. et al., 2017, ApJ, 848, L23
Freiburghaus C., Rosswog S., Thielemann F.-K., 1999, ApJ, 525, L121
Fulbright J. P., 2000, AJ, 120, 1841
Giacobbo N., Mapelli M., 2018, MNRAS, 480, 2011
Graur O. et al., 2011, MNRAS, 417, 916
Heringer E., Pritchet C., Kezwer J., Graham M. L., Sand D., Bildfell C., 2016, ApJ, 834, 15
Honda S., Aoki W., Kajino T., Ando H., Beers T. C., Izumiura H., Sadakane K., Takada-Hidai M., 2004, ApJ, 607, 474
Hotokezaka K., Kiuchi K., Kyutoku K., Muranushi T., Sekiguchi Y.-i., Shibata M., Taniguchi K., 2013, Phys. Rev. D, 88, 044026
Howard W., Mathews G., Takahashi K., Ward R., 1986, ApJ, 309, 633

Downloaded from https://academic.oup.com/mnras/article/503/1/1/6127305 by inaf user on 05 August 2021

Ishimaru Y., Wanajo S., Aoki W., Ryan S. G., 2003, ApJ, 600, L47
Ivanova N., Heinke C., Rasio F. A., Belczynski K., Fregeau J., 2008, MNRAS, 386, 553
Kalogera V. et al., 2004, ApJ, 601, L179
Karlsson T., Gustafsson B., 2005, A&A, 436, 879
Koch A., Edvardsson B., 2002, A&A, 381, 500
Komiya Y., Shigeyama T., 2016, ApJ, 830, 76
Korobkin O., Rosswog S., Arcones A., Winteler C., 2012, MNRAS, 426, 1940
Maeder A., Meynet G., 1989, A&A, 210, 155
Maoz D., Badenes C., 2010, MNRAS, 407, 1314
Maoz D., Mannucci F., 2012, PASA, 29, 447
Matteucci F., Greggio L., 1986, A&A, 154, 279
Matteucci F., Panagia N., Pipino A., Mannucci F., Recchi S., Della Valle M., 2006, MNRAS, 372, 265
Matteucci F., Romano D., Arcones A., Korobkin O., Rosswog S., 2014, MNRAS, 438, 2177
McWilliam A., 1998, AJ, 115, 1640
Mennekens N., Vanbeveren D., 2014, A&A, 564, A134
Mösta P., Ott C. D., Radice D., Roberts L. F., Schnetter E., Haas R., 2015, Nature, 528, 376
Nishimura N., Takiwaki T., Thielemann F.-K., 2015, ApJ, 810, 109
Oechslin R., Janka H. T., Marek A., 2007, A&A, 467, 395
Panov I. V., Korneev I. Y., Thielemann F. K., 2008, Astron. Lett., 34, 189
Perego A., Rosswog S., Cabezón R. M., Korobkin O., Käppeli R., Arcones A., Liebendörfer M., 2014, MNRAS, 443, 3134
Rodney S. A. et al., 2014, AJ, 148, 13
Roederer I. U., Preston G. W., Thompson I. B., Shectman S. A., Sneden C., Burley G. S., Kelson D. D., 2014, AJ, 147, 136
Scalo J. M., 1986, Fundamentals of cosmic physics, 11, p. 1
Schönrich R. A., Weinberg D. H., 2019, MNRAS, 487, 580
Shao Y., Li X.-D., 2018, MNRAS, 477, L128
Shen S., Cooke R. J., Ramirez-Ruiz E., Madau P., Mayer L., Guedes J., 2015, ApJ, 807, 115
Siegel D. M., Barnes J., Metzger B. D., 2019, Nature, 569, 241
Simonetti P., Matteucci F., Greggio L., Cescutti G., 2019, MNRAS, 486, 2896
Symbalisty E., Schramm D. N., 1982, Astrophys. Lett., 22, 143
Tanvir N. R., Levan A. J., Fruchter A. S., Hjorth J., Hounsell R. A., Wiersema K., Tunnicliffe R. L., 2013, Nature, 500, 547
Tauris T. et al., 2017, ApJ, 846, 170
Thornton K., Gaudlitz M., Janka H.-T., Steinmetz M., 1998, ApJ, 500, 95
Totani T., Morokuma T., Oda T., Doi M., Yasuda N., 2008, PASJ, 60, 1327
Wanajo S., Kajino T., Mathews G. J., Otsuki K., 2001, ApJ, 554, 578
Wanajo S., , Janka H. T., Müller B., Kubono S., 2011, J. Phys. Conf. Ser., 312, 042008
Wanajo S., Sekiguchi Y., Nishimura N., Kiuchi K., Kyutoku K., Shibata M., 2014, ApJ, 789, L39
Winteler C., Kaeppeli R., Perego A., Arcones A., Vasset N., Nishimura N., Liebendoerfer M., Thielemann F.-K., 2012, ApJ, 750, L22
Woolf V. M., Tomkin J., Lambert D. L., 1995, ApJ, 453, 660
Woosley S., Wilson J., Mathews G., Hoffman R., Meyer B., 1994, ApJ, 433, 229
Yoon S. C., Langer N., Norman C., 2006, A&A, 460, 199

This paper has been typeset from a TEX/LATEX file prepared by the author.

Downloaded from https://academic.oup.com/mnras/article/503/1/1/6127305 by inaf user on 05 August 2021